Environ Monit Assess (2019) 191: 180
https://doi.org/10.1007/s10661-019-7262-1

Assessing the ecological risks from hydrocarbons in the marine coastal sediments of Jeddah, Red Sea

Bandar A. Al-Mur

Received: 11 October 2018 / Accepted: 23 January 2019 / Published online: 22 February 2019

Abstract The Red Sea is a unique aquatic environment, and it is host to highly biodiverse marine organisms. This body of water occurs along the western side of Saudi Arabia, which is one of the largest producers of crude oil in the world. Thus, the sea's contamination by oil pollutants could pose a large problem and is a major concern in the region. The samples were analyzed to determine their polycyclic aromatic hydrocarbon (PAH) speciation and assess the associated ecological risk to the coastal environment of the Red Sea. The geographical distribution of the 16 total PAHs by concentration (range and average values in ng g^{-1} dry wt.) occurred in the following order: the northern region (1169.8 to 2742.0; 2083) < the southern region (1971.4 to 3003.4; 2493) < the middle region (2222.0 to 2930.6; 2599). The PAHs with two, three, four, five, and six rings make up 7.0%, 13.0%, 70.0%, and 10.0% of the total PAHs, respectively. The diagnostic ratio results showed that the PAHs may be attributed to petrogenic and pyrogenic sources. The PAH concentrations were considered toxic when their levels ranged from 119 to 491 ng toxic equivalent g^{-1} dry wt. According to the mean range of PAH effects (the mean effect range median quotient values), the ecological risk posted by the investigated sediments was lower than 0.1, denoting a toxicity effect with a probability of 11%. The analysis of PAHs highlighted that the sampling sites were low priority sites, and their PAHs may not cause acute biological damage.

Keywords Jeddah · Red Sea · Sediment · PAHs · Ecological risk

B. A. Al-Mur (✉)
Department of Environmental Sciences, Faculty of Meteorology, Environment and Arid Land Agriculture, King Abdulaziz University, Jeddah, Saudi Arabia
e-mail: Balmur@kau.edu.sa

Introduction

The abundance of polycyclic aromatic hydrocarbons (PAHs) in coastal marine waters and their risks to human health have drawn the attention of scientists and decision makers. The PAHs in marine sediments have accumulated from both natural and human sources such as the incomplete burning of crude oil and fossil fuels. PAHs are associated with several human diseases, such as carcinogenesis, mutagenesis, and hemolytic properties (Kamal et al. 2014). PAHs are of great concern to nearby urban populations (Szabová et al. 2008). Many organic pollutants, including PAHs, are released into marine environments due to the combustion of wood, oil, coal, gas, and garbage (Liu et al. 2008; Gorleku et al. 2014). These substances come from municipal effluents, atmospheric fallout, automobile exhaust, urban runoff, industrial effluents, and oil spillage (Anyakora et al. 2011; Battalwar et al. 2012; Roozbeh et al. 2012). Coastal areas and inland waters usually act as receptors for vast amounts of many pollutants from the surrounding petroleum products.

The Red Sea has a surface water temperature reaching 31 °C in summer and 26 °C in winter with a

high salinity of about 40% (Rifaat 1996; Ghandour et al. 2014). In addition, the study area is usually hot with a humid climate and a little precipitation between 50 and 100 mm per year (Basaham 2008). Generally, the sediments' mineralogy of the Jeddah coast was found to be muddy sediments in the southern and carbonate in the northern area (Al-Washmi 1999).

The Kingdom of Saudi Arabia is one of the largest producers of crude oil in the world. The city of Jeddah, which is located on the eastern shore of the Red Sea, is the most industrialized city in Saudi Arabia (Al-Mur et al. 2017). Contamination by oil pollutants is a primary concern in the region. The discharge of polycyclic aromatic hydrocarbons into the marine environment represents a risk to human health due to the carcinogenic impact of crude oil. Humans are at a higher level on the food chain, and therefore, they accumulate polycyclic aromatic hydrocarbons as they consume marine organisms (Fisler 1987). The stress on the Jeddah coastal area is very deep, with a population of ca. 3.4 million. It is considered to be the most significant commercial center, as it combines severe socioeconomic activities and built-up area. Due to rapid and diverse growth, the coastal city of Jeddah shows an environmental deterioration, such as an increased number of vehicles which led to an increased rate of air quality deterioration. Power plant, desalination plant, and refinery are the biggest stationary PAH sources in Jeddah. Thus, the Jeddah coastal area is suffering from heavy loads of many environmental problems such as anthropogenic inputs from industrial and sewage effluents, shipping activities, spillage, atmospheric fallout, coastal activities, and natural oil seeps. The levels of PAHs in marine sediment, seawater, and food are affected by the presence of PAH in street dust (Shabbaj et al. 2018).

Due to contamination stress on the Jeddah coast, several monitoring studies are investigated including nutrients, aliphatic and total hydrocarbons, heavy metals, and polychlorinated biphenyls, where most of these contaminants were found at high levels (Ali et al. 2011; El Sayed and Basaham 2004; Turki 2006; Al-Farawati 2010; El-Maradny et al. 2015; Rasiq et al. 2018). However, studies on the Red Sea sediments are still few and there are defects in the sedimentology and geochemical studies in the coast of Jeddah, Red Sea. To the best of our knowledge, a little information about the individual PAHs has been recorded in Jeddah coastal area sediments. Therefore, due to the increasing human activities and the rapid development in the area, the present study will be very important and necessary. Accordingly, the present study considered a detailed account of the spatial variation of the individual PAHs in the marine coastal sediments of Jeddah, Red Sea coast, Saudi Arabia, and can be used as baseline information for assessing the PAH contamination load in this region. The aims of this study are to identify the origin and different concentrations of PAHs in the marine coastal deposits of the Jeddah area, to measure the degree of PAH contamination in these marine coastal deposits, and to determine the potential risk posed by PAHs both to the marine coastal ecosystem of the Red Sea and to the human health.

Materials and methods

Strategy for sample collection

To measure the hydrocarbon pollution levels in the Red Sea along Jeddah, Saudi Arabia, sediment samples were taken from the bottom sediments of the marine coastal water, near the shore of Jeddah, during March of 2018 (Fig. 1). Eighteen bottom sediment samples were recovered from the coast of Jeddah. These samples were collected from three sites. The first site is called "Salman Gulf" and located in the northern region of Jeddah and includes six samples (1, 2, 3, 4, 5, and 6). The second site is downtown area and includes the middle region which contains four samples (7, 8, 9, and 10). The third location of sampling stations is Al-Khumrah, which contains eight samples (11, 12, 13, 14, 15, 16, 17, and 18), representing the southern region of Jeddah. These locations were selected to cover the entire coastal region of the study area. The sediment samples were recovered from the water using a grab sampler, and the upper 3 cm of the samples was scraped and placed in a container for this study. These locations were selected to cover the entire coastal region of the study area. Approximately 100 g of surface sediment was collected and placed into clean, dark glass jars; kept in an insulated icebox; and stored in a dark place with a temperature under − 4 °C. At the laboratory, the sediment samples were immediately stored in aluminum containers. After that, they were dried at room temperature, and then a grain-size analysis was performed according to Folk (1974). In addition, the organic carbon content (total, TOC%) of the studied sediment samples was measured using the methodology of Gaudette et al. (1974). The total

carbonate was determined by the titration technique described by Molina (1974).

Extraction of sediment samples, GC-MS analysis, and validation studies

The extraction of the PAHs from the sediment samples was conducted and analyzed by GC-MS. The quality assurance and quality control (QA/QC) procedures used for the GC-MS analysis are described in Wade et al. (1988). These procedures included an analysis of duplicates, laboratory blanks, matrix spikes, and certified reference material (Wade and Cantillo 1994).

The ultrasonic extraction method is applied for the extraction of PAHs in sediments. At room temperature, dichloromethane is used to extract PAHs for 30 min, and then the sample is shaken, ultrasonication is performed for 30 min, and finally, the sample is filtered through a glass wool pipette. The extracted hydrocarbons were concentrated via evaporator rotation until reaching 3–6 ml, and then they were evaporated to 0.5 ml with pure nitrogen. Different cleanup techniques have been developed to remove potential interference prior to GC-MS analysis. Cleanup procedures are applied by many researchers to enhance the sensitivity of the methods via silica/alumina chromatographic columns, and sulfur is removed using activated copper powder.

The PAHs in the sediment samples were determined using gas chromatography mass spectrometry (Agilent 7000 GC-MS/MS, USA). The procedure was started by injecting an extract with a volume of 1 μl at 270 °C in splitless mode. A mixture of PAH standards was used to quantify 16 PAH compounds depending on their retention times. The preparation and analysis of the sediment samples were performed for the following 16 PAH compounds: naphthalene (Naph, *m/z* 128), acenaphthylene (Acthy, *m/z* 152), acenaphthene (Ace, *m/z* 154), fluorine (Fl, *m/z* 166), phenanthrene (Phen, *m/z* 178), anthracene (Ant, *m/z* 178), fluoranthene (Flu, *m/z* 202), pyrene (Pyr, *m/z* 202), benzo[a]anthracene (BaA, *m/z* 228), chrysene (Chry, *m/z* 228), benzo[b]fluoranthene (BbF, *m/z* 252), benzo[k]fluoranthene (BkF, *m/z* 252), benzo[a]pyrene (BaP, *m/z* 252), benzo[ghi]perylene (BghiP, *m/z* 278), indeno[1,2,3-cd]pyrene (InP, *m/z* 278), and dibenzo[a,h]anthracene (DBahA, *m/z* 278).

The sediment that was previously extracted by the ultrasonication system was used for extraction recovery. The standard was spiked to give final concentrations over ranges of 1–20 ng g^{-1}, 10–200 ng g^{-1}, and 100–2000 ng g^{-1} for the PAH mixture ($n = 3$ each concentration).

The method validation process was designed with attention to its accuracy, precision, evaluation of linearity, limit of quantification (LOQ), and limit of detection (LOD). Its accuracy and precision were evaluated by measuring three replicates of each QC sample. All the pesticide grade solvents were purchased from Merck. The 16 PAH compounds are considered by the United States Environmental Protection Agency (USEPA) as PAH priority pollutants. The LODs and LOQs were determined using the signal-to-noise ratio.

Results and discussion

Grain-size analyses and organic carbon and $CaCO_3$ contents of the sediments

The results of the studied sediment characteristics, grain-size analysis, TOC%, and carbonate ($CaCO_3$) contents are illustrated in Table 1. The distribution/abundance of fine sediments (clay and silt) and sand in the near-shore deposits of the Jeddah coastal zone was 0.0–39.0% for clay + silt and 61.0–100.0% for sand. The texture of the sediments taken from the 18 locations along the Jeddah field area revealed that some of the sediment is fine sand (stations 1–3, 7, 8, and 13–15). All sediments in the area of the study revealed a high content of sand fractions (61–100%). Thus, the dominant fraction in the collected samples was the sand (Table 1). In addition, the result of clay plus silt fractions fluctuated between 0.0 and 39%. Therefore, the sediments along the study area stations contain varieties of sediment types including coarse sand (stations 5, 6, 9, 11, 12, 16, and 17), coarse and fine sand (stations 4, 10, and 18), fine sand (stations 1, 3, and 13–15), and very fine sand (stations 2, 7, and 8).

The level of total organic carbon (TOC%) ranged from 0.26 to 1.44%, and the average value was 0.95% of the high concentration values; more than 1% was found in the area from station 8 to station 18, except St. 9 (0.95%), and the low concentration value was recorded in the area from stations 1 to 7 (their contents ranged between 0.26 and 0.94%) (Table 1). The moderately high TOC concentrations may be a result of the direct discharge of domestic and industrial wastes (Pekey et al. 2004). The carbonate concentration (as $CaCO_3$) in the sediment samples ranged from 5.03 to

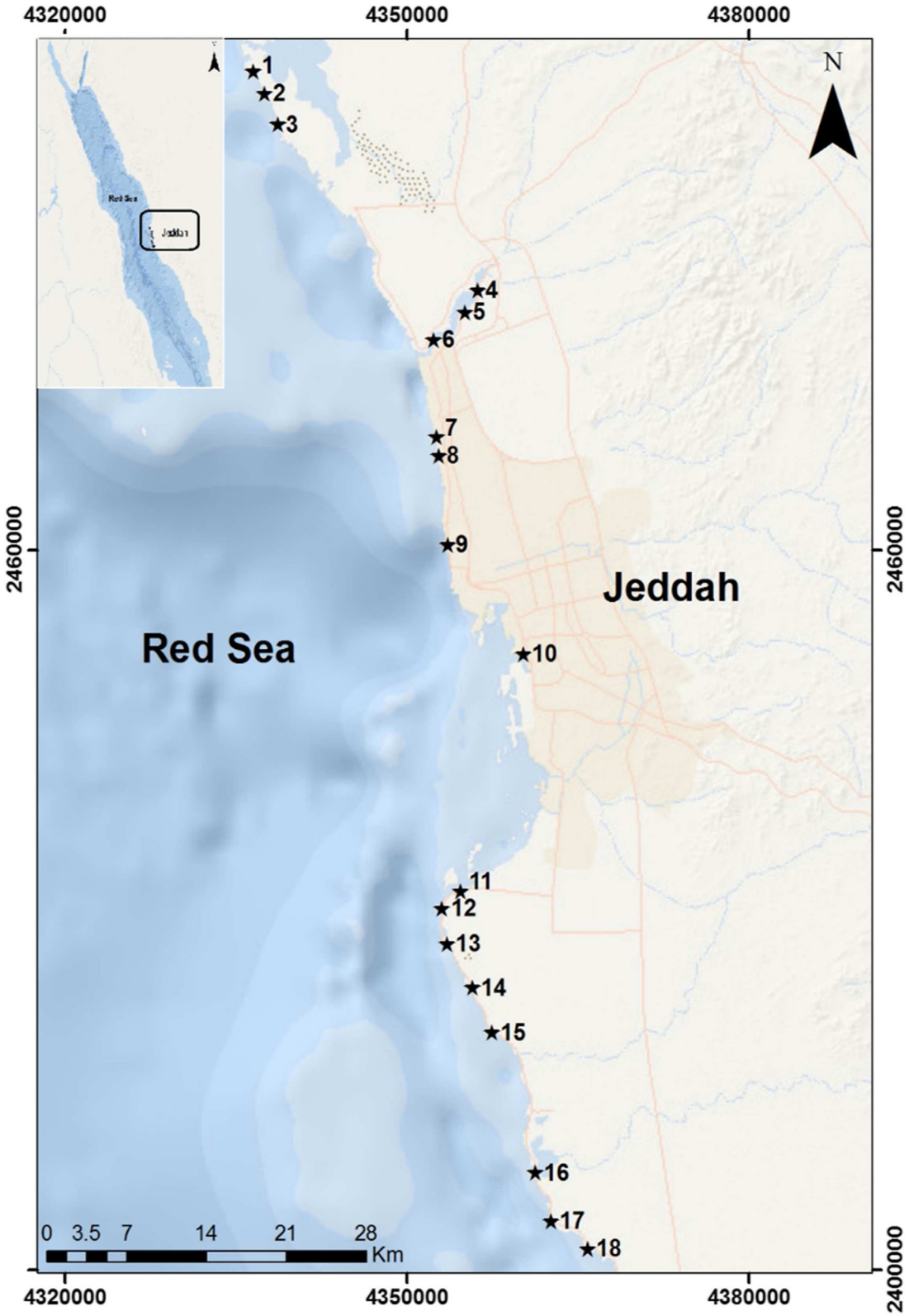

Fig. 1 Location of sampling points

Table 1 Characterization of the sediments along the study area

St.	Locations		Grain size		TOC (%)	$CaCO_3$ (%)	Sediment type
	Latitude (N)	Longitude (E)	Sand (%)	Silt + clay (%)			
1	21.876617	38.972557	98.0	2.0	0.35	25.80	Fine sand
2	21.866340	38.975300	61.0	39.0	0.26	5.03	Very fine sand
3	21.845668	38.993319	95.8	4.2	0.70	21.44	Fine sand
4	21.751210	39.132770	96.2	3.8	0.66	29.36	Coarse and fine sand
5	21.736623	39.122015	100.0	0.0	0.60	54.55	Coarse sand
6	21.720934	39.113549	100.0	0.0	0.63	53.34	Coarse sand
7	21.574080	39.109060	86.0	14.0	0.94	54.49	Very fine sand
8	21.520035	39.130082	96.0	4.0	1.03	31.45	Very fine sand
9	21.509899	39.160771	100.0	0.0	0.95	18.00	Coarse sand
10	21.473369	39.163543	100.0	0.0	1.09	16.59	Coarse and fine sand
11	21.332450	39.119300	100.0	0.0	1.09	42.60	Coarse sand
12	21.320480	39.104820	98.5	1.5	1.18	46.47	Coarse sand
13	21.295800	39.108900	96.1	3.9	1.23	35.36	Fine sand
14	21.265594	39.128387	85.5	14.5	1.44	29.50	Fine sand
15	21.234010	39.144280	98.6	1.4	1.16	21.97	Fine sand
16	21.136170	39.178060	97.3	2.7	1.37	30.05	Coarse sand
17	21.102150	39.190420	100.0	0.0	1.31	57.33	Coarse sand
18	21.082930	39.219490	94.9	5.1	1.30	61.37	Coarse and fine sand
Min			61.0	0.00	0.26	5.03	
Max			100.0	39.0	1.44	61.37	
Ave.			93.3	6.8	0.95	35.06	

61.37% as found in station 2 and station 18, respectively, with a mean value of 35.06%.

PAH analysis

The concentrations of the 16 recorded PAHs in the studied surficial sediments from the 18 sampling sites that were collected from the Jeddah coast are listed in Table 2 and shown in Fig. 2. The concentrations of the recorded ∑16 PAHs in the sediments from the study area were in the following range: from 1909.6 ng g^{-1} dry wt. in station 4 to 2893 ng g^{-1} dry wt. in station 11. The observed differences in the ∑16 PAH concentrations in the sediments along the study area were related to the differences in the human activities and discharged pollutants.

As shown in Table 2, the individual PAHs were dominated by Flu, Pyr, and Chry, ranging from 199.3 to 970.7 ng g^{-1} dry wt., from 268.7 to 788.7 ng g^{-1} dry wt., and from 286 to 710.7 ng g^{-1} dry wt. for the three PAHs, respectively. However, the concentrations of BaP (104–390 ng g^{-1} dry wt.) and Phen (90.5–292.2 ng g^{-1} dry wt.) were also high at the study area. The amounts of the other PAH compounds found in the studied sediments of the coastal zone of the Jeddah coast were low, ranging from the LOD for DBahA and InP to 184.6 ng g^{-1} dry wt. for BaA, and their presumed contribution to the ∑16 PAH concentrations in the samples is low.

According to the present results, Table 2 shows that the concentrations of low molecular weight PAHs (two to three rings, low PAHs (LPAHs)) in the sediment samples are lower than those of the high molecular weight compounds (four to six rings, high PAHs (HPAHs)). The HPAHs were more dominant in the study area than LPAHs (Fig. 2), with total concentration values (ng g^{-1} dry wt.) ranging from 978.5 to 2482 for the former (HPAHs) (Table 2) and from 191.4 to 601.9 for the latter (LPAHs). The total concentration of the

Table 2 Sixteen individual PAH concentrations (ng g^{-1} dry wt.) in the surface sediments from Jeddah, Red Sea

Compound	Rings	Stations in the northern region						Stations in the middle region				Stations in the southern region							
		1	2	3	4	5	6	7	8	9	10	11	12	13	14	15	16	17	18
Naph	2	8.8	15.3	21.8	16.6	17.7	11.2	30.4	32.8	37.7	15.1	12.5	9.9	34.8	40.8	38.0	45.5	60.3	32.8
Acthy	2	12.5	28.9	40.6	42.1	60.1	82.4	86.3	64.0	50.2	47.8	32.0	29.9	40.6	38.0	44.7	50.4	64.0	73.8
Ace	2	38.0	62.7	87.6	118.6	127.9	142.0	112.1	92.6	81.1	61.4	50.2	88.9	71.8	64.0	55.4	63.4	95.7	96.7
Fl	3	17.7	34.8	71.0	75.7	68.1	47.8	38.0	43.7	37.2	49.9	89.4	81.1	39.5	40.8	29.6	36.9	46.3	56.2
Phen	3	90.5	119.1	170.8	172.1	216.8	229.3	292.2	288.6	240.2	224.1	188.2	267.8	231.9	280.8	286.0	265.2	187.2	169.0
Ant	3	23.9	29.4	36.9	24.2	21.8	29.6	42.9	49.9	32.5	40.0	38.2	43.7	33.3	50.2	55.9	42.1	29.6	38.0
Flu	4	199.3	390.0	580.7	459.3	849.3	589.3	572.0	398.7	970.7	832.0	1066	771.3	554.7	745.3	823.3	398.7	398.7	294.7
Pyr	4	268.7	459.3	589.3	364.0	658.7	702.0	658.7	424.7	372.7	485.3	355.3	294.7	485.3	589.3	684.7	719.3	788.7	537.3
BaA	4	52.0	78.0	39.0	95.3	121.3	95.3	39.0	40.7	70.2	72.8	81.5	123.1	58.1	184.6	131.7	150.8	100.5	119.6
Chry	4	286.0	355.3	303.3	329.3	416.0	468.0	502.7	710.7	615.3	546.0	589.3	338.0	381.3	511.3	468.0	476.7	329.3	320.7
BbF	5	17.3	29.5	97.1	29.5	50.3	0.0	0.0	38.1	27.7	0.0	0.0	0.0	18.2	19.9	15.6	10.4	100.5	29.5
BkF	5	27.7	13.0	0.0	0.0	0.0	0.0	9.5	12.1	13.9	0.0	0.0	0.0	0.0	0.0	0.0	26.9	19.1	14.7
BaP	5	116.1	294.7	199.3	164.7	104.0	121.3	147.3	121.3	199.3	312.0	390.0	476.7	208.0	164.7	104.0	138.7	147.3	234.0
DBahA	5	0.0	0.0	0.0	0.0	0.0	0.0	0.0	0.0	0.0	0.0	0.0	0.0	0.0	0.0	0.0	0.0	0.0	0.0
BghiP	6	11.3	29.5	13.0	18.2	0.0	0.0	15.6	37.3	48.5	0.0	0.0	12.1	15.6	13.9	0.0	0.0	13.0	10.4
InP	6	0.0	0.0	0.0	0.0	0.0	0.0	0.0	0.0	10.4	0.0	0.0	16.5	10.4	0.0	0.0	0.0	0.0	0.0
TPAH		1169.8	1939.4	2250.5	1909.6	2712.1	2518.4	2546.7	2355.1	2807.7	2686.5	2893	2554	2183	2744	2737	2425	2380	2027
LPAH[a]		191.4	290.2	428.7	449.3	512.5	542.4	601.9	571.5	478.9	438.4	410.5	521.3	451.9	514.5	509.6	503.6	483.1	466.4
HPAH[b]		978.5	1649.3	1821.7	1460.3	2199.6	1976.0	1944.8	1783.6	2328.7	2248.1	2482	2032	1732	2229	2227	1921	1897	1561

[a] Low PAHs: naphthalene (Naph), acenaphthylene (Acthy), acenaphthene (Ace), fluorene (Fl), phenanthrene (Phen), and anthracene (Ant)

[b] High PAHs: fluoranthene (Flu), pyrene (Pyr), benzo[a]anthracene (BaA), chrysene (Chry), benzo[b]fluoranthene (BbF), benzo[k]fluoranthene (BkF), benzo[a]pyrene (BaP), dibenzo[a,h]anthracene (DBahA), benzo[ghi]perylene (BghiP), indeno[1,2,3-cd]pyrene (InP)

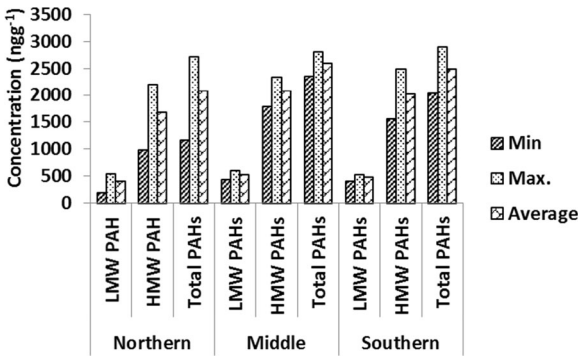

Fig. 2 Min., max., and average of total PAH, LMW PAH, and HMW PAH concentrations (ng g^{-1} dry wt.) in the surface sediments from Jeddah City, Red Sea

LPAHs (a range between 191.4 and 601.9 ng g^{-1} dry wt.) is recorded for 88% of the total samples.

The concentrations of LPAHs in the studied sediments can be arranged as follows: Naph (8.8–60.3 ng g^{-1}) < Ant (21.8–55.9 ng g^{-1}) < Fl (17.7–89.4 ng g^{-1}) < Acthy (12.5–86.3 ng g^{-1}) < Ace (38.3–142 ng g^{-1}) < Phen (90.5–292.2 ng g^{-1}). Flu, Pyr, and Chry were the most contaminations of the HPAHs, with contents ranging from 199.3 to 1066.0 ng g^{-1} dry wt., from 268.7 to 788.7 ng g^{-1} dry wt., and from 286.0 to 710.7 ng g^{-1} dry wt., respectively.

These compounds contributed averages of 25%, 22%, and 19%, respectively, to the ∑16 PAHs along the study area. The concentration values for Flu (199.3–1066 ng g^{-1} dry wt.) showed that it was the dominant component, followed by Pyr (268.7–702.0 ng g^{-1} dry wt.) and Chry (286.0–710.7 ng g^{-1} dry wt.) (Table 2). The wide variation between the LPAH and HPAH concentrations was recorded in the study area. Previous studies revealed that most HPAHs are carcinogenic (Wang et al. 2015). However, this result indicated that the sediments in the present study close to the Jeddah coastal zone were derived from a mixture of sources from petrogenic and pyrogenic origins.

The difference in the contaminant abundance of the PAH compounds may be partially ascribed to differences in their molecular weights and the occurrence of bacterial activities. PAH compounds such as naphthalene and phenanthrene are characterized by lower molecular weights, so they are readily degraded in the sediments. However, pyrene, fluoranthene, benzo[a]anthracene, and benzo[a]pyrene are more refractory, with their high molecular weights, so they are not easily degraded (Obayori and Salam 2010).

In the present study, the ∑16 PAHs yielded a total concentration of 1169.8–3003.4 ng g^{-1} dry wt. This total concentration was compared with those of the previous studies on the Red Sea and with coastal marine sediments from around the world. The analysis and comparison of the total PAH levels in this study showed that their concentrations were lower than the PAHs in Guanabara Bay, Rio de Janeiro, Brazil (77–7751 ng g^{-1} dry wt.) (da Silva et al. 2007); in Vhembe District, South Africa (27,100–55,930 ng g^{-1} dry wt.) (Edokpayi et al. 2016); in the Mediterranean Sea (13.5–22,600 ng g^{-1} dry wt.) (Barakat et al. 2011); in Boston Harbor, USA (7300–358,000 ng g^{-1} dry wt.) (Keshavarzifard et al. 2014); in the Red Sea, Gulf of Suez (ND–1513 ng g^{-1} dry wt.) (Abdallah et al. 2016); in the Red Sea, Saudi Arabia (900–23,000 ng g^{-1} dry wt.) (Fowler et al. 1993); and along the Egyptian Red Sea coast (132–5182 ng g^{-1} dry wt.; 1628 ng g^{-1} dry wt.) (El Nemr et al. 2014). The concentration levels of ∑16 PAHs observed in this study were highly relative to those reported for the Red Sea, Saudi Arabia (39–1729 ng g^{-1} dry wt.) (Rasiq et al. 2018). Additionally, they are four- to six-fold higher concentrations compared with those from the Gulf of Suez, the Gulf of Aqaba, the western side (Egyptian) of the Red Sea coast (0.74–456.91 ng g^{-1} dry wt.) (Salem et al. 2014), and the Red Sea (Gulf of Aden) (2.2–604 ng g^{-1} dry wt.; 82.4 ng g^{-1} dry wt.) (Mostafa et al. 2009). Compared with the other areas, the concentration of ∑16 PAHs in the concentrations of the Jeddah coastal zone was increased significantly by two- to three-fold relative to those reported in Todos os Santo Bay, Brazil (11.45–1825 ng g^{-1} dry wt.) (Nascimento et al. 2017); in Langkawi Island (869–1637 ng g^{-1} dry wt.) (Nasher et al. 2013); and along the eastern Guangdong coast of South China (29.4–815.5 ng g^{-1} dry wt.) (Gu et al. 2016).

In this study, the relative proportions of PAHs with different numbers of rings varied among the studied sediments along the coastal zone of Jeddah, and the PAHs containing four rings dominated, followed by three-ring PAHs. Moreover, all the sites were dominated by HPAHs (high molecular weight compounds) such as Pyr, Flu, BaA, BkF, Chry, BbF, BaP, DBahA, BghiP, and InP (Table 2). The PAHs in the studied sediments primarily consisted of compounds with four, five, and six rings (high molecular weights). The results indicate that the HPAH concentration increased four times compared with the LPAH level. The PAH concentration is influenced directly or indirectly by the industrial and

Table 3 Individual PAH diagnostic ratio values and their possible sources

Diagnostic ratio	Petrogenic	Pyrogenic	References
Ant/Ant + Phen	< 0.1	> 0.1	Budzinski et al. (1997); Brandli et al. (2007)
Flu/Flu + Pyr	< 0.4	> 0.4	Yang et al. (2017); Brandli et al. (2007)
Phen/Phen + Ant	< 0.7	> 0.7	Alves et al. (2001); Sienra et al. (2005)
BaA/BaA + Chry	< 0.2	> 0.2	Li et al. (2016); Tobiszewski and Namieśnik (2012)
LMW/HMW	> 1	< 1	Nasher et al. (2013)
Flu/Pyr	< 1	> 1	Kuo et al. (2012)
BaA/Chry	< 0.4	> 0.9	Kuo et al. (2012)
Phen/Ant	> 10	< 10	Kuo et al. (2012)

sewage wastewater from Jeddah. Moreover, the major source of PAHs for most stations could be the discharge of industrial and sewage wastewater and urban emissions from the surrounding area. The PAHs formed at high temperatures acquire condensed structures with four, five, and six rings, and they represent the majority of PAH input from industrial runoff and urban wastewaters.

Possible sources and origins of PAH pollutants

PAH source identification is vital for understanding the transport of these hydrocarbons in the studied environments (Wang et al. 2009). The ratios and concentrations of many PAH compounds are generally utilized to distinguish among their possible sources (Yunker et al. 2002; Katsoyiannis and Breivik 2014). The PAH ratios are used for interpreting the PAH sources, composition, and diagenesis.

In the sediments from the study area, different criteria for diagnosing various individual PAH ratios are used as indicators of their origin and for evaluating their possible sources (Table 3, Fig. 3a–c). In this study, many diagnostic ratios such as the Phen/(Ant + Phen), Flu/(Pyr + Flu), and BaA/(BaA + Chry) ratios were investigated to uncover the potential origin of PAHs found in the Jeddah coastal zone area.

The individual PAH ratios (Phen/Ant and Flu/Pyr) were calculated (Yunker et al. 2002; Liu et al. 2009; Yim et al. 2011; Kuo et al. 2012; Xie et al. 2012; Li et al. 2016), and the ratios of Ant/Ant + Phen, Flu/Flu + Pyr, and ∑LMW/∑HMW were also identified. In addition, a plot of isomeric ratios (a comparison) for Ant/(Ant + Phen) against Flu/(Flu + Pyr) has been used to successfully differentiate the PAH sources (e.g., Jiang et al. 2009; Martins et al. 2010; Xue et al. 2013).

The petrogenic inputs of the PAHs are categorized by a high Phen/Ant ratio (Wang et al. 2011), while the occurrence of high levels of four-ring and five-ring hydrocarbons is an indication of a mixture produced by burning fossil fuels (Yang et al. 2005; Kuo et al. 2012). In Fig. 3, the recorded result shows that the ratios of Phen/Ant and Flu/Pyr may denote the PAH contamination sources. Hence, the ratios of Phen/Ant < 10 and Flu/Pyr > 1 could suggest possible contamination as a result of pyrolytic activities (Kuo et al. 2012). Additionally, the results show that the contamination of eight stations (1, 2, 3, 6, 7, 8, 17, and 18) may be related to petrogenic sources because the Flu/Pyr ratio is less than 1, while the Flu/Pyr ratio is greater than 1, as shown in stations 4, 5, and 9–15, which have values of 1.26, 1.29, 2.61, 1.72, 3.00, 2.62, 1.14, 1.26, and 1.20, respectively, and are primarily contaminants of pyrolytic origin (Fig. 3).

As shown in Fig. 3, the ratio of BaA/Chry is < 0.9, and it ranged from 0.06 to 0.37. This finding indicates petrogenic contamination and suggests the presence of PAHs with a petrogenic source in the sediment samples taken from the Jeddah coastal zone.

The petrogenic PAHs are rich in lower molecular weight compounds (LPAHs), which could be easily weathered when compared with the higher molecular weight PAHs (HPAHs). The distribution of LPAHs and HPAHs may be used as another indicator of the origin of the PAHs (Abdallah et al. 2016). Previous studies have suggested that high ratios of ∑LPAHs/∑HPAHs (larger than 1.0) could indicate a predominance of PAHs with petrogenic sources, while a low ratio of ∑LPAHs/∑HPAHs, of less than 1, frequently suggests PAHs of

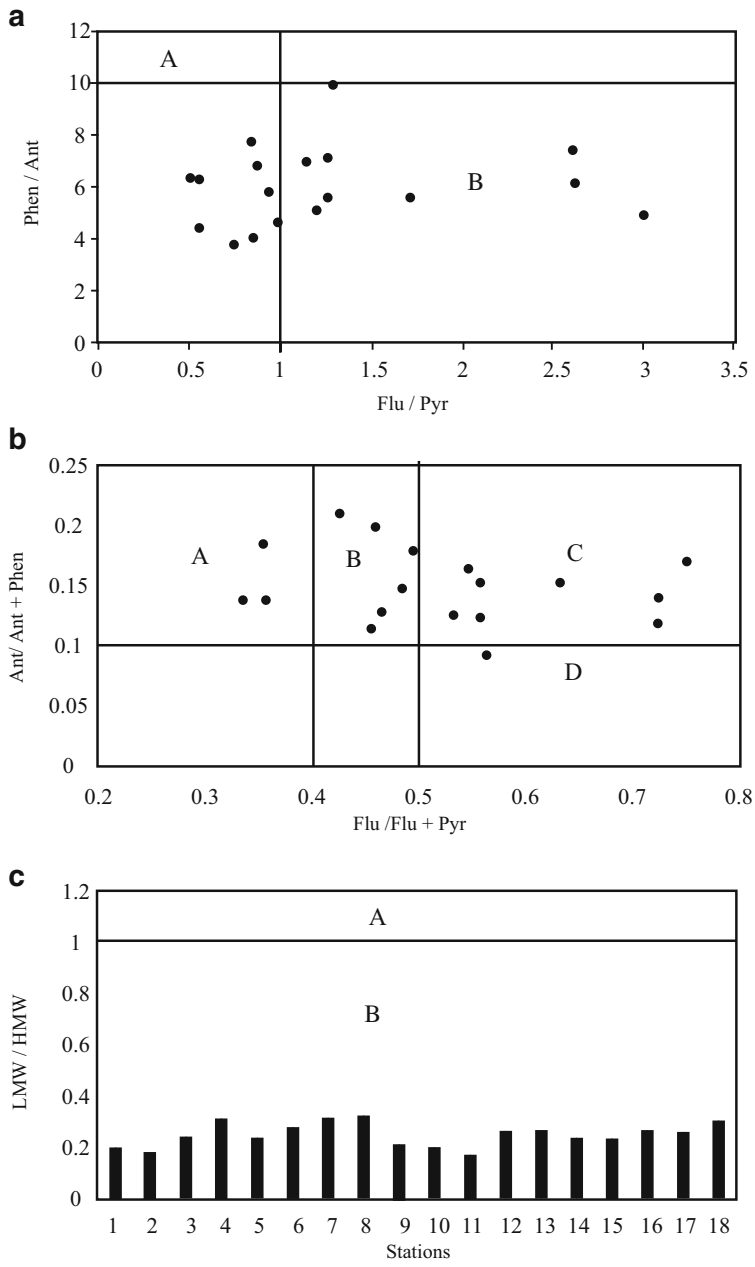

Fig. 3 Cross plot for the isomeric ratios of **a** Cross plot for isomeric ratios of Flu/Pyr vs. Phen/Ant (A: typical of petrogenic; B: typical of pyrogenic) in surface sediments from Jeddah, Red Sea, **b** Cross plot for isomeric ratios of Flu/Flu + Pyrvs. Ant/Ant + Phen (A: typical of petrogenic; B: petrogenic combustion; C: Grass, Wood, Coal combustion and D: petrogenic), and **c** Cross plot for LMW / HMW ratios of PAHs (A: typical of petrogenic; B: typical of pyrolytic) in surface sediments from Jeddah, Red Sea

pyrolytic origin (Ke et al. 2002; de Luca et al. 2004). Therefore, all the sediment samples in the study area, that is, in these regions (∑LPAHs/∑HPAHs) with low values, indicate that the PAHs are from pyrolytic sources (Fig. 3).

With some exceptions, such as station 5, the Ant/(Ant + Phen) ratio in the study area sediments was > 0.1 (0.1–0.21), which suggests that the source of the PAHs was from pyrogenic sources as a result of biomass combustion (Nasher et al. 2013). The LPAH/HPAH ratio gave values of < 1 (0.17–0.32) for all the studied sites, supporting the notion that the source of the PAHs in this area could have originated from biomass combustion. Moreover, the use of the Flu/(Flu + Pyr) ratio yielded

values ranging from 0.43 to 0.75 at most of the study sites, confirming the occurrence of pyrogenic sources. Otherwise, when the Flu/(Flu + Pyr) ratio is smaller than 0.4, the PAHs are implied to have originated from the use of petroleum products, which have been recorded at three sites in the eastern region (stations 16–18). The values of Ant/(Ant + Phen) were 0.10–0.21, all of which are higher than 0.1. In general, the source of PAHs at those sites could be attributed to pyrogenic activities.

Tobiszewski and Namieśnik (2012) declared that when the BaA/(BaA + Chry) ratio is 0.2–0.35, these PAHs could have coal burning sources, while a ratio of > 0.35 could indicate vehicular emission sources. In the present study, the BaA/(BaA + Chry) ratio was approximately 0.1–0.27, or all the values were less than 0.35. The above findings could suggest that the PAHs in the studied sediments may have primarily originated from the combustion of petroleum compounds (Fig. 3).

The Phen/(Phen + Ant) ratio could also be an indicator showing a potential origin of burning biomass (> 0.7) or petrogenic hydrocarbons (< 0.7) (Alves et al. 2001; Sienra et al. 2005). In this study, the value of Phen/(Phen + Ant) ranged from 0.336 to 0.909 (Fig. 3), which indicates biomass burning, which could, in turn, represent the primary source of PAH pollution found in the study area from stations 1 to 12, where the ratio was less than 0.7, and it may be related to petrogenic hydrocarbons (< 0.7) at the other six stations (stations 13 to 18).

Yang et al. (2017) mentioned that when the diagnostic ratio of Flu/(Flu + Pyr) is less than 0.4, the source of PAHs could be unburned petroleum, which is a primary source of PAH pollution. Additionally, they suggested that a 0.4–0.5 ratio could denote that the source is liquid fossil fuel, while a ratio > 0.5 could indicate that wood or coal could be the sources of the PAHs. In this study, the Flu/(Flu + Pyr) ratio in the Jeddah coastal zone was higher than 0.5 for all the studied samples except in stations 16–18 (Fig. 3), which indicates a significant influence from wood and coal combustion through the Flu/(Flu + Pyr) values.

Assessment of ecological risk from the individual PAHs

In the present study, three approaches to the sediment quality guidelines (SQGs) were used to assess the ecological risks of individual PAHs. They are the effect range low (ERL), the effect range median (ERM), and the total toxic BaP equivalent (total TEQ_{xcarc}). In addition, the mean effect range median quotient (M-ERM-q) was used to assess both the toxicity levels and ecological risks of the PAHs. These approaches are appropriate methodologies for assessing the marine sediment quality, for ranking them as the recipients of potentially low or high impacts (Fairey et al. 2001). The concentrations of the recorded PAHs are listed with their ERL and ERM values in Table 4. The results revealed that the individual PAHs and the total PAH concentrations for several sites from the Jeddah coastal zone sediments were above the ERL but below the ERM. The individual PAH concentrations showed that the Ace concentration exceeded the ERL in all the study areas (stations 1–18). In the study area, the Acthy concentration exceeded the ERL at stations 5–10 and stations 16–18. The concentration of Chry exceeded the ERL at 12 stations, from stations 5–16. The Fl concentration exceeded the ERL in the middle and southern regions at stations 7–18. The Flu concentration exceeded the ERL in the middle and southern regions at stations 9–15. The levels for both the Phen and Pyr concentrations exceeded the ERL at stations 7–10 and 15–17, respectively. In general, the PAHs with potential impacts were Acthy, Ace, Fl, Flu, Pyr, and Chry.

In this study, the individual PAHs with values below the ERM are considered not to be highly toxic. However, several PAH compounds at some sites had values below the ERM and above the ERL, which could occasionally cause negative toxic effects. Another technique (M-ERM-q) was used to determine the predicted biological toxicity effects of the PAHs on the marine organisms. The estimation of the M-ERM-q for all the PAHs was performed using the equation proposed by Feng et al. (2015) as follows:

$$\mathrm{ERM{-}q} = C_i/\mathrm{ERM}_x$$

$$\mathrm{M{-}ERM{-}q} = \sum(C_i/\mathrm{ERM}_x)/N$$

where C_i is the PAH level, ERM_x N is the number of PAHs, and ERM is the value of the same target of the PAH. According to a previous study, in the toxicity data recorded by Long et al. (1995), the M-ERM-q values can be subdivided into four categories depending on their probability of toxicity as follows: ≤ 0.1, 0.11 to 0.5, 0.51 to 1.5, and > 1.5 indicate toxicity probabilities of 11%, 30%, 46%, and 75%, respectively. This toxicity probability percentage could sort the studied sites into low, medium-low, medium-high, and high priorities,

Table 4 Comparison of individual PAH concentrations (ng g^{-1} dry weight) in the surface sediments from Jeddah, Saudi Arabia (Red Sea), with toxicity guidelines of PAH components

PAHs	SQGs (ng g^{-1}) dry wt.				Study area					
					Northern region		Middle region		Southern region	
	ERL	ERM	TEL	PEL	Min.	Max.	Min.	Max.	Min.	Max.
Naph	160	2100	50	400	8.8	21.8	15.1	37.7	9.9	60.3
Acthy	44	640	5.87	128	12.5	82.4	47.8	86.3	29.9	73.8
Ace	16	500	10	100	38.0	142.0	61.4	112.1	50.2	96.7
Fl	19	540	15	180	17.7	75.7	37.2	49.9	29.6	89.4
Phen	240	1500	86.7	544	90.5	229.3	224.1	292.2	169.0	286.0
Ant	853	1100	46.9	245	21.8	36.9	32.5	49.9	29.6	55.9
Flu	600	5100	113	1494	199.3	849.3	398.7	970.7	294.7	1066.0
Pyr	665	2600	153	1398	268.7	702.0	372.7	658.7	294.7	788.7
BaA	261	1600	74.8	693	39.0	121.3	39.0	72.8	58.1	184.6
Chry	384	2800	18	846	286.0	468.0	502.7	710.7	320.7	589.3
BbF	320	1880	NA	NA	0.0	97.1	0.0	38.1	0.0	100.5
BkF	280	1620	NA	NA	0.0	27.7	0.0	13.9	0.0	26.9
BaP	430	1600	88.8	763	104.0	294.7	121.3	312.0	104.0	476.7
DBahA	63.4	260	6.22	135	0.0	0.0	0.0	0.0	0.0	0.0
BghiP	NA	NA	NA	NA	0.0	29.5	0.0	48.5	0.0	15.6
InP	NA	NA	NA	NA	0.0	0.0	0.0	10.4	0.0	16.5
∑PAHs	4000	44,792			1169.1	2742.0	2222.0	2930.6	1971.4	3003.4

NA not available data (*ERL*) effect range low, (*ERM*) effect range median, (*TEL*) threshold effect level, (*PEL*) probable effect level

respectively. According to these categories, the M-ERM-q values in the studied sediments from each site along the Jeddah coastal zone area ranged from 0.037 to 0.087 with a mean of 0.07 (Table 5). The results of this study are lower than 0.1 with an 11% probability of toxicity. The study locations are also classified as low-priority sites.

The third tool used in the present study is the toxic equivalency factor (TEF_{xcarc}). It was used by Nadal et al. (2004) to estimate the benzo[a]pyrene equivalent (BaP_{eq}) doses of other PAHs and to quantify their carcinogenicity relative to benzo[a]pyrene. By using the equation by Chen and Chen (2011) and Nasher et al. (2013), the potential toxicity of the studied sediments was then calculated using the total toxic BaP equivalent (TEQ_{xcarc}) for all the concentrations of an individual PAH (CPAHs). This equation is as follows:

$$\mathrm{TEQ}^{\mathrm{carc}} = \sum_i C_i \times \mathrm{TEF}_i^{\mathrm{carc}}$$

where C_i is equal to the concentration of an individual CPAH (ng g^{-1} dry wt.) and TEF_{xcarc} (toxic equivalency factor) is equal to the toxic factor of this CPAH relative to the BaP according to USEPA (1993) and Savinov et al. (2003). The TEF_{xcarc} values were calculated for BaA, BbF, BkF, InP, BaP, Chry, BghiP, and DBahA as 0.1, 0.1, 0.01, 1, 0.1, 0.001, 0.01, and 1.0, respectively. In this study, the concentrations of eight individual PAHs of the abovementioned compounds were combined into one toxic level for each site via the corresponding TEF_{xcarc}.

The total TEQ_{xcarc} in the study area (18 sediment samples) ranged from 119 to 491 ng g^{-1} BaP_{eq} (Table 5). The range and total average concentrations of potentially carcinogenic ∑8 PAHs (CPAH in ng g^{-1} dry wt.) for the three regions were the following: from 510 to 800 (661 ± 104) for the northern region, from 714 to 985 (881.6 ± 218.9) for the middle region, and from 691 to 1060.8 (832.7 ± 219) for the southern region. Their contributions to the total ∑16 PAHs were in the ranges 25.5–43.6%, 28.00–40.80%, and 26.30–37.8%

Table 5 Total ∑16 PAHs, total ∑8 $PAHs_{carc}$, contribution %, and total M-ERM-q

Stations	Total ∑16 PAHs	Total ∑8 $PAHs_{carc}$	Contribution %	M-ERM-q	Total TEQ_{xcarc}
Northern region					
1	1169.9	510.4	43.6	0.037	124
2	1939.4	800	41.2	0.062	306
3	2250.5	651.7	29	0.074	213
4	1909.6	637	33.4	0.07	178
5	2742	691.6	25.5	0.087	122
6	2518.4	684.6	27.2	0.086	131
Min–max	1169–2742	510.4–800.0	25.5–43.6	0.037–0.087	122–306
Average ± SD	2055 ± 591	661 ± 104	33.63 ± 7.51	0.07 ± 0.02	188 ± 75
Middle region					
7	2546.7	714.1	28	0.084	152
8	2222	960.2	40.8	0.078	130
9	2930.6	985.3	35.1	0.079	211
10	2686.5	930.8	34.6	0.079	320
Min–max	2222–2930	714.1–985.3	28.00–40.80	0.078–0.084	130–320
Average ± SD	2589 ± 668	881.6 ± 218.9	34.55 ± 8.95	0.080 ± 0.020	210 ± 79
Southern region					
11	3003.4	1060.8	36.7	0.083	399
12	2553.6	966.4	37.8	0.085	491
13	2183.5	691.6	31.7	0.068	217
14	2743.6	894.4	32.6	0.081	186
15	2736.9	719.3	26.3	0.078	119
16	2425	803.5	33.1	0.077	156
17	2380.2	709.7	29.8	0.08	168
18	1971.4	728.9	36	0.075	249
Min–max	1971–3003	691.6–1060.8	26.30–37.8	0.068–0.085	119–491
Average ± SD	2497 ± 646	832.7 ± 219.1	32.81 ± 8.43	0.078 ± 0.019	260 ± 111

for the three regions, respectively (Table 5). The PAHs and their average contents relative to the total TEQ_{xcarc} vary according to this order: BaA (8.3–23.7%), BbF (6.0–20.5%), DBahA (3.1–21.9%), Chry (1.8–8.9%), BkF (0.0–4.4%), BaP (0.0–2.9%), BghiP (0.00–0.00%), and InP (0.00–0.00%). This trend suggests that more individual attention should be paid to BaA, BbF, DBahA, and Chry.

In comparison to the TEQ_{xcarc} for the studied sediments in the northern, middle, and southern regions of the study area, the TEQ_{xcarc} of the southern region was in the range from 119 to 491 ng TEQ g^{-1} d.w. with an average of 260 ± 111 ng TEQ g^{-1} d.w., having slightly higher levels of total TEQ_{xcarc} than those recorded in the northern region, which ranged between 122 and 306 ng TEQ g^{-1} d.w., with an average of 188 ± 75 ng TEQ g^{-1} d.w. The TEQ_{xcarc} of the middle region was 130–320 ng TEQ g^{-1} d.w., with an average of 210 ± 79 ng TEQ g^{-1} d.w. (Table 5).

Matrix correlation between sediment characteristics and PAHs

Several studies showed that the physicochemical characteristic such as TOC and grain size are two important controlling factors for the sorption and distribution of PAHs in sediments (Qiao et al. 2006; Malik et al. 2011; Agarwal and Bucheli 2011; Timoney and Lee 2011; Feng et al. 2015). In the present study, the correlations between PAH concentrations in sediments with TOC and grain size are shown in Table 6. TOC was positively significantly correlated with total PAHs ($r = 0.0.508$),

Table 6 Pearson correlation between sediment characteristics and PAHs in the surface sediments from Jeddah, Red Sea

	Naph	Acthy	Ace	Fl	Phen	Ant	Flu	Pyr	BaA	Chry	BbF
Naph	1										
Acthy	0.327	1									
Ace	− 0.07	0.727**	1								
Fl	− 0.38	− 0.04	0.333	1							
Phen	0.392	0.427*	0.178	− 0.04	1						
Ant	0.344	0.102	− 0.31	− 0.12	0.730**	1					
Flu	− 0.14	− 0.07	− 0.06	0.411*	0.416*	0.24	1				
Pyr	0.574**	0.629**	0.348	− 0.22	0.334	0.158	− 0.07	1			
BaA	0.297	− 0.05	− 0.04	0.062	0.286	0.262	0.166	0.33	1		
Chry	0.154	0.266	− 0.08	− 0.09	0.616**	0.490*	0.489*	− 0.02	− 0.08	1	
BbF	0.185	0.362	0.463*	0.262	− 0.17	− 0.24	− 0.1	0.434*	− 0.31	− 0.26	1
BkF	0.166	− 0.37	− 0.471*	− 0.4	− 0.34	− 0.2	− 0.454*	− 0.02	0.188	− 0.29	− 0.22
BaP	− 0.414*	− 0.39	− 0.27	0.562**	− 0.1	0.099	0.369	− 0.532*	− 0	− 0.05	− 0.15
BghiP	− 0.19	− 0.08	− 0.23	0.133	0.043	0.038	0.539*	− 0.38	− 0.33	0.715**	− 0.17
TPAH	0.235	0.333	0.143	0.309	0.718**	0.479*	0.835**	0.342	0.322	0.628**	0.053
LPAH	0.396	0.729**	0.574**	0.199	0.875**	0.502*	0.311	0.494*	0.238	0.465*	0.164
HPAH	0.17	0.194	0.014	0.307	0.606**	0.425*	0.891**	0.268	0.313	0.609**	0.018
Sand	0.076	0.146	0.147	0.272	0.232	0.017	0.286	0.025	0.032	0.132	0.096
Silt + clay	− 0.11	− 0.12	− 0.11	− 0.23	− 0.24	− 0.08	− 0.17	− 0.01	− 0.02	− 0.07	− 0.06
TOC	0.666**	0.217	− 0.17	0.061	0.625**	0.643**	0.213	0.286	0.477*	0.286	− 0.12
$CaCO_3$	0.13	0.614**	0.588**	0.323	0.171	− 0.11	− 0.06	0.352	0.173	− 0.14	0.313

	BkF	BaP	BghiP	TPAH	LPAH	HPAH	Sand	Silt + c lay	TOC	$CaCO_3$
Naph										
Acthy										
Ace										
Fl										
Phen										
Ant										
Flu										
Pyr										
BaA										
Chry										
BbF										
BkF	1									
BaP	− 0.21	1								

Table 6 (continued)

	BkF	BaP	BghiP	TPAH	LPAH	HPAH	Sand	Silt + c lay	TOC	$CaCO_3$
BghiP	− 0.28	0.346	1							
TPAH	− 0.486*	0.19	0.406*	1						
LPAH	− 0.495*	− 0.16	− 0.05	0.697**	1					
HPAH	− 0.436*	0.263	0.488*	0.982**	0.55**	1				
Sand	0.202	− 0.11	0.022	0.244	0.28	0.210	1			
Silt + clay	− 0.25	0.149	0.09	− 0.14	− 0.27	− 0.095	− 0.98**	1		
TOC	0.027	0.138	− 0.05	0.508*	0.553**	0.445*	0.349	− 0.372	1	
$CaCO_3$	− 0.09	− 0.07	− 0.38	0.158	0.474*	0.058	0.380	− 0.36	0.298	1

**Correlation is significant at the 0.01 level (one-tailed)

*Correlation is significant at the 0.05 level (one-tailed)

LPAHs ($r = 0.553$), HPAHs ($r = 0.445$), and the individual PAHs (Naph, Phen, Ant, and BaA; $r = 0.666$, 0.625, 0.643, and 0.477, respectively). In the previous studies, the LPAHs are found in great affinity for autochthonous and allochthonous organic matters from plankton origin and terrestrial origin, respectively (Countway et al. 2003).

In contrast, there was no significant correlation between total PAHs and individual PAH concentrations with both sand and silt + clay percentages, suggesting that grain size is only a minor factor influencing PAH accumulation and may be derived from combustion processes (Lohmann et al. 2005). This result was in agreement with those reported by Timoney and Lee (2011), who did not observe a correlation between PAH concentration and sediment grain size.

Analysis of the relationship between the individual PAHs was performed and determined the r value of the correlation. Between Phe and each of Ant, Flu, Chry, total PAH, low PAH, and high PAH, the coefficients were $r = 0.73$, 0.416, 0.616, − 0.718, 875, and 0.606, respectively. However, a linear distribution with a significant correlation was observed between Flu and both Fl and BaP ($r = 0.414$ and $r = 0.562$, respectively) and between Acthy and each of Ace, Phen, Pyr, and low PAH ($r = 0.0.727$, 0.427, 0.629, and 0.729, respectively) and between Naph and both Pyr and BaP ($r = 0.574$ and $r = 0.414$, respectively). The relationship between Ace and both BbF ($r = 0.463$) and low PAH ($r = 0.574$) was recorded (Table 6). The relationship between Chry and each of BghiP, total PAH, low PAH, and high PAH was 0.715, 0.628, 0.465, and 0.609, respectively.

The values between the individual PAHs suggested that these compounds respond unequally to weathering processes, as photo-oxidation. Similarly, they can undergo distinct processes in the environment, which may change the characteristics of these PAH sources. On the other hand, the linearity of the correlation between the isomers evaluated may suggest that these compounds are under similar environmental processes or have the same behavior, maintaining the information about their origin (Qiao et al. 2006).

Conclusions

Sediment contaminants including 16 individual polycyclic aromatic hydrocarbons (PAHs) were analyzed in 18 surficial sediment samples recovered

from the coastal area of Jeddah, Saudi Arabia. The highest concentration of total PAHs was observed in the middle region and the southern region due to heavy loads of anthropogenic inputs from industrial and sewage effluents, shipping activities, spillage, atmospheric fallout, coastal activities, and natural oil seeps. The relationship between the PAH concentration and physicochemical characteristic showed a positive correlation between the concentrations of TOC and each of the concentration of total PAHs ($r = 0.508$), low molecular weight PAHs (LPAHs; $r = 0.553$), high molecular weight PAHs (HPAHs; $r = 0.445$), and the individual PAHs (Naph, Phen, Ant, and BaA; $r = 0.666$, 0.625, 0.643, and 0.477, respectively). These correlations are probably due to the same inputs of PAHs and TOC. In contrast, there was no significant correlation between total PAHs and individual PAH concentrations with both sand and silt + clay percentages, suggesting that grain size is only a minor factor influencing PAH accumulation.

Acknowledgments The author gratefully acknowledges the Deanship of Scientific Research (DSR) for its technical and financial support.

Funding information This work was supported by the Deanship of Scientific Research (DSR), King Abdulaziz University, Jeddah, under grant no. D-067-155-1439.

References

Abdallah, R. I., Khalil, N. M., & Roushdy, M. I. (2016). Monitoring of pollution in sediments of the coasts in Egyptian Red Sea. *Egyptian Journal of Petroleum, 25*(1), 133–151.

Agarwal, T., & Bucheli, T. D. (2011). Is black carbon a better predictor of polycyclicaromatic hydrocarbon distribution in soils than total organic carbon? *Environmental Pollution, 159*, 64–70.

Al-Farawati, R. (2010). Environmental conditions of the coastal waters of southern Corinche, Jeddah, eastern Red Sea: physico-chemical approach. *Australian Journal of Basic and Applied Sciences, 4*, 3324.

Ali, A., Elazein, E., & Alian, M. (2011). Investigation of heavy metals pollution in water, sediment and fish at Red Sea-Jeddah coast-KSA at two different locations. *Journal of Applied Environmental Biological Sciences, 1*, 630.

Al-Mur, B. A., Quicksall, A. N., & Al-Ansari, A. M. A. (2017). Spatial and temporal distribution of heavy metals in coastal core sediments from the Red Sea, Saudi Arabia. *Oceanologia, 59*(3), 262–270.

Alves, C., Pio, C., & Duarte, A. (2001). Composition of extractable organic matter of air particles from rural and urban Portuguese areas. *Atmospheric Environment, 35*(32), 5485–5496.

Al-Washmi, H. A. (1999). Sedimentological aspects and environmental conditions recognized from the bottom sediments of Al-Kharrar lagoon, eastern Red Sea coastal plain, Saudi Arabia. *Journal of King Abdulaziz University, 10*, 71–87.

Anyakora, C. H., Coker, H., & Arbabi, M. (2011). Application of polynuclear aromatic hydrocarbons in chemical fingerprinting: the Niger Delta case study. *Iranian Journal of Environmental Health Science & Engineering, 8*(1), 75–84.

Barakat, A. O., Mostafa, A., Wade, T. L., Sweet, S. T., & El Sayed, N. B. (2011). Distribution and characteristics of PAHs in sediments from the Mediterranean coastal environment of Egypt. *Marine Pollution Bulletin, 62*(9), 1969–1978.

Basaham, A. S. (2008). Mineralogical and chemical composition of the mud fraction from the surface sediments of Sharm Al-Kharrar, a Red Sea coastal lagoon. *Oceanologia, 50*(4), 557–575.

Battalwar, D. G., Yenkie, M. K. N., Meshram, S. U., & Puri, P. J. (2012). Studies on presence of PAHs in ambient air of Nagpur City (India). *Rasayan Journal of Chemistry, 5*(3), 345–350.

Brandli, R. C., Bucheli, T. D., Kupper, T., Mayer, J., Stadelmann, F. X., & Tarradellas, J. (2007). Fate of PCBs, PAHs and their source characteristic ratios during composting and digestion of source-separated organic waste in full-scale plants. *Environmental Pollution, 148*, 520–528.

Budzinski, H., Jones, I., Bellocq, J., Pierrad, C., & Garrigues, P. (1997). Evaluation of sediment contamination by polycyclic aromatic hydrocarbons in the Gironde estuary. *Marine Chemistry, 58*, 85–97.

Chen, C.-W., & Chen, C.-F. (2011). Distribution, origin, and potential toxicological significance of polycyclic aromatic hydrocarbons (PAHs) in sediments of Kaohsiung Harbor, Taiwan. *Marine Pollution Bulletin, 63*(5–12), 417–423.

Countway, R. E., Dickhut, R. M., & Canuel, E. (2003). Polycyclic aromatic hydrocarbon (PAH) distributions and associations with organic matter in surface waters of the York River, VA estuary. *Organic Geochemistry, 34*, 209–224.

da Silva, T. F., Azevedo, D. D. A., & Neto, F. R. D. A. (2007). Distribution of polycyclic aromatic hydrocarbons in surface sediments and waters from Guanabara Bay, Rio de Janeiro, Brazil. *Journal of the Brazilian Chemical Society, 18*(3), 628–637.

de Luca, G., Furesi, A., Leardi, R., Micera, G., Panzanelli, A., Piu, P. C., & Sanna, G. (2004). Polycyclic aromatic hydrocarbons assessment in the sediments of the Porto Torres Harbor (northern Sardinia, Italy). *Marine Chemistry, 86*(1–2), 15–32.

Edokpayi, J., Odiyo, J., Popoola, O., & Msagati, T. (2016). Determination and distribution of polycyclic aromatic hydrocarbons in rivers, sediments and wastewater effluents in Vhembe District, South Africa. *International Journal of Environmental Research and Public Health, 13*(4), 387.

El Nemr, A., El-Sadaawy, M. M., Khaled, A., & El-Sikaily, A. (2014). Distribution patterns and risks posed of polycyclic

aromatic hydrocarbons contaminated in the surface sediment of the Red Sea coast (Egypt). *Desalination and Water Treatment, 52*(40–42), 7964–7982.

El Sayed, M. A., & Basaham, A. S. (2004). Speciation and mobility of some heavy metals in the coastal sediments of Jeddah, eastern Red Sea. *Arab Gulf Journal of Scientific Research, 22*, 226.

El-Maradny, A. A., Turki, A. J., Shaban, Y. A., & Sultan, K. M. (2015). Levels and distribution of polychlorinated biphenyls in Jeddah coastal sediments, Red Sea, Saudi Arabia. *Journal of the Chemical Society of Pakistan, 37*(3), 599.

Fairey, R., Long, E. R., Roberts, C. A., Anderson, B. S., Phillips, B. M., Hunt, J. W., Puckett, H. R., & Wilson, C. J. (2001). An evaluation of methods for calculating mean sediment quality guideline quotients as indicators of contamination and acute toxicity to amphipods by chemical mixtures. *Environmental Toxicology and Chemistry, 20*, 2276–2286.

Feng, J., Xi, N., Zhang, F., Zhao, J., Hu, P., & Sun, J. (2015). Distributions and potential sources of polycyclic aromatic hydrocarbons in surface sediments from an emerging industrial city (Xinxiang). *Environmental Monitoring and Assessment, 188*(1), 1–14.

Fisler, R. (1987). *Polycyclic aromatic hydrocarbon hazards to fish, wildlife and invertebrate: a synoptic review*. Laurel: U. S. Fish and Wildlife Service Patuxent Wildlife Research Center.

Folk, R. L. (1974). *Petrology of sedimentary rocks*. Austin: Hemphill.

Fowler, S. W., Readman, J. W., Oregioni, B., Villeneuve, J. P., & McKay, K. (1993). Petroleum hydrocarbons and trace metals in nearshore gulf sediments and biota before and after the 1991 war: an assessment of temporal and spatial trends. *Marine Pollution Bulletin, 27*, 171–182.

Gaudette, H., Flight, W., Toner, L., & Folger, D. (1974). An inexpensive titration method for the determination of organic carbon in recent sediments. *Journal of Sedimentary Research, 44*(1), 249–253.

Ghandour, I. M., Basaham, A. S., Al-Washmi, H. A., & Masuda, H. (2014). Natural and anthropogenic controls on sediment composition of an arid coastal environment: Sharm Obhur, Red Sea, Saudi Arabia. *Environmental Monitoring and Assessment, 186*(3), 1465–1484.

Gorleku, M. A., Carboo, D., Palm, L. M. N., Quasie, W. J., & Armah, A. K. (2014). Polycyclic aromatic hydrocarbons (PAHs) pollution in marine waters and sediments at the Tema Harbour, Ghana. *Academia Journal of Environmental Sciences, 2*(7), 108–115.

Gu, Y.-G., Ke, C.-L., Liu, Q., & Lin, Q. (2016). Polycyclic aromatic hydrocarbons (PAHs) in sediments of Zhelin Bay, the largest mariculture base on the eastern Guangdong coast, South China: characterization and risk implications. *Marine Pollution Bulletin, 110*(1), 603–608.

Jiang, J.-J., Lee, C.-L., Fang, M.-D., & Liu, J. T. (2009). Polycyclic aromatic hydrocarbons in coastal sediments of southwest Taiwan: an appraisal of diagnostic ratios in source recognition. *Marine Pollution Bulletin, 58*(5), 752–760.

Kamal, A., Malik, R. N., Martellini, T., & Cincinelli, A. (2014). PAH exposure biomarkers are associated with clinico-chemical changes in the brick kiln workers in Pakistan. *Science of the Total Environment, 490*, 521–527.

Katsoyiannis, A., & Breivik, K. (2014). Model-based evaluation of the use of polycyclic aromatic hydrocarbons molecular diagnostic ratios as a source identification tool. *Environmental Pollution, 184*, 488–494.

Ke, L., Wong, T. W. Y., Wong, Y. S., & Tam, N. F. Y. (2002). Fate of polycyclic aromatic hydrocarbon (PAH) contamination in a mangrove swamp in Hong Kong following an oil spill. *Marine Pollution Bulletin, 45*(1–12), 339–347.

Keshavarzifard, M., Zakaria, M. P., Hwai, T. S., Yusuff, F. F. M., Mustafa, S., Vaezzadeh, V., Magam, S. M., Masood, N., Alkhadher, S. A. A., & Abootalebi-Jahromi, F. (2014). Baseline distributions and sources of polycyclic aromatic hydrocarbons (PAHs) in the surface sediments from the Prai and Malacca Rivers, Peninsular Malaysia. *Marine Pollution Bulletin, 88*(1–2), 366–372.

Kuo, J.-Y., Ko, F.-C., Cheng, J.-O., Meng, P.-J., Li, J.-J., & Hung, C.-C. (2012). Environmental assessment of polycyclic aromatic hydrocarbons in the surface sediments of a remote region on the eastern coast, Taiwan. *Environmental Monitoring and Assessment, 184*(5), 2967–2979.

Li, Z., Chen, L., Liu, S., Ma, H., Wang, L., An, C., & Zhang, R. (2016). Characterization of PAHs and PCBs in fly ashes of eighteen coal-fired power plants. *Aerosol and Air Quality Research, 16*(12), 3175–3186.

Liu, G., Niu, Z., van Niekerk, D., Xue, J., & Zheng, L. (2008). Polycyclic aromatic hydrocarbons (PAHs) from coal combustion: emissions, analysis, and toxicology. In D. M. Whitacre (Ed.), *Reviews of environmental contamination and toxicology* (pp. 1–28). New York: Springer.

Liu, A., Lang, Y., Xue, L., & Liu, J. (2009). Ecological risk analysis of polycyclic aromatic hydrocarbons (PAHs) in surface sediments from Laizhou Bay. *Environmental Monitoring and Assessment, 159*(1–4), 429–436.

Lohmann, R., Macfarlane, J. K., & Gschwend, P. M. (2005). Importance of black carbon tosorption of native PAHs, PCBs, and PCDDs in Boston and New York harbor sediments. *Environmental Science & Technology, 39*, 141–148.

Long, E. R., Macdonald, D. D., Smith, S. L., & Calder, F. D. (1995). Incidence of adverse biological effects within ranges of chemical concentrations in marine and estuarine sediments. *Environmental Management, 19*(1), 81–97.

Malik, A., Verma, P., Singh, A. K., & Singh, K. P. (2011). Distribution of polycyclic aromatic hydrocarbons in water and bed sediments of the Gomti River, India. *Environmental Monitoring and Assessment, 172*(1), 529–545.

Martins, C. C., Bícego, M. C., Rose, N. L., Taniguchi, S., Lourenço, R. A., Figueira, R. C. L., Mahiques, M. M., & Montone, R. C. (2010). Historical record of polycyclic aromatic hydrocarbons (PAHs) and spheroidal carbonaceous particles (SCPs) in marine sediment cores from Admiralty Bay, King George Island, Antarctica. *Environmental Pollution, 158*(1), 192–200.

Molina, B. F. (1974). A rapid and accurate method for the analysis of calcium carbonate in small samples. *Journal of Sedimentary Petrology, 44*(2), 589–590.

Mostafa, A. R., Wade, T. L., Sweet, S. T., Al-Alimi, A. K. A., & Barakat, A. O. (2009). Distribution and characteristics of polycyclic aromatic hydrocarbons (PAHs) in sediments of Hadhramout coastal area, Gulf of Aden, Yemen. *Journal of Marine Systems, 78*(1), 1–8.

Nadal, M., Schuhmacher, M., & Domingo, J. L. (2004). Levels of PAHs in soil and vegetation samples from Tarragona County, Spain. *Environmental Pollution, 132*(1), 1–11.

Nascimento, R. A., de Almeida, M., Escobar, N. C. F., Ferreira, S. L. C., Mortatti, J., & Queiroz, A. F. S. (2017). Sources and distribution of polycyclic aromatic hydrocarbons (PAHs) and organic matter in surface sediments of an estuary under petroleum activity influence, Todos os Santos Bay, Brazil. *Marine Pollution Bulletin, 119*(2), 223–230.

Nasher, E., Heng, L. Y., Zakaria, Z., & Surif, S. (2013). Assessing the ecological risk of polycyclic aromatic hydrocarbons in sediments at Langkawi Island, Malaysia. *The Scientific World Journal, 2013*, 1–13.

Obayori, O. S., & Salam, L. B. (2010). Degradation of polycyclic aromatic hydrocarbons: role of plasmids. *Scientific Research and Essays, 5*(25), 4093–4106.

Pekey, H., Karakaş, D., Ayberk, S., Tolun, L., & Bakoğlu, M. (2004). Ecological risk assessment using trace elements from surface sediments of İzmit Bay (northeastern Marmara Sea) Turkey. *Marine Pollution Bulletin, 48*(9–10), 946–953.

Qiao, M., Wang, C., Huang, S., Wang, D., & Wang, Z. (2006). Composition, sources, and potential toxicological significance of PAHs in the surface sediments of the Meiliang Bay, Taihu Lake, China. *Environment International, 32*, 28–33.

Rasiq, K. T., El-Maradny, A., Bashir, M. E., & Orif, M. (2018). Polycyclic aromatic hydrocarbons (PAHs) in surface sediments of two polluted lagoons in Saudi Arabia. *Polish Journal of Environmental Studies, 27*(1), 275–285.

Rifaat, A. R. (1996). Metal composition of recent carbonate sediments off Jeddah, Kingdom of Saudi Arabia. *Marine Scienes-Ceased lssuerg, 17*(1), 1–2.

Roozbeh, M., Iraj, F., & Ehsan, A. (2012). Contamination of polycyclic aromatic hydrocarbons in surface sediments of Khure-Musa estuarine, Persian Gulf. *Journal of Fish and Marine Sciences, 4*(2), 136–141.

Salem, D. M. S. A., Morsy, F. A.-E. M., El Nemr, A., El-Sikaily, A., & Khaled, A. (2014). The monitoring and risk assessment of aliphatic and aromatic hydrocarbons in sediments of the Red Sea, Egypt. *The Egyptian Journal of Aquatic Research, 40*(4), 333–348.

Savinov, V. M., Savinova, T. N., Matishov, G. G., Dahle, S., & Næs, K. (2003). Polycyclic aromatic hydrocarbons (PAHs) and organochlorines (OCs) in bottom sediments of the Guba Pechenga, Barents Sea, Russia. *Science of the Total Environment, 306*(1–3), 39–56.

Shabbaj, I. I., Alghamdi, M. A., & Khoder, M. I. (2018). Street dust—bound polycyclic aromatic hydrocarbons in a Saudi coastal city: status, profile, sources, and human health risk assessment. *International Journal of Environmental Research and Public Health, 15*(11), 2397. https://doi.org/10.3390/ijerph15112397.

Sienra, M. D. R., Rosazza, N. G., & Préndez, M. (2005). Polycyclic aromatic hydrocarbons and their molecular diagnostic ratios in urban atmospheric respirable particulate matter. *Atmospheric Research, 75*(4), 267–281.

Szabová, E., Zeljenková, D., Nesčáková, E., Šimko, M., & Turecký, L. (2008). Polycyclic aromatic hydrocarbons and occupational risk factor. *Reproductive Toxicology, 26*(1), 74.

Timoney, K. P., & Lee, P. (2011). Polycyclic aromatic hydrocarbons increase in Athabasca River Delta sediment: temporal trends and environmental correlates. *Environmental Science & Technology, 45*, 4278–4284.

Tobiszewski, M., & Namieśnik, J. (2012). PAH diagnostic ratios for the identification of pollution emission sources. *Environmental Pollution, 162*, 110–119.

Turki, A. J. (2006). Concentration of some heavy metals in surface sediments of a coastal Red Sea lagoon receiving domestic sewage, *Journal of Egyptian Academic Society for Environmental Development, (D – Environmental Studies). 7* (3): 21–40.

USEPA. (1993). *Provisional guidance for quantitative risk assessment of polycyclic aromatic hydrocarbons, EPA/600/R-93/089*. Washington, DC: Office of Research and Development, US Environment Protection Agency.

Wade, T. L., & Cantillo, A. Y. (1994). Use of standards and reference materials in the measurement of chlorinated hydrocarbon residues. Chemistry workbook. NOAA Technical Memorandum NOS ORCA 77. Silver Spring: US Department of Commerce.

Wade, T. L., Atlas, E. L., Brooks, J. M., Kennicutt, M. C., Fox, R. G., Sericano, J., Garcia-Romero, B., & DeFreitas, D. (1988). NOAA Gulf of Mexico status and trends program: trace organic contaminant distribution in sediments and oysters. *Estuaries, 11*(3), 171–179.

Wang, L., Yang, Z., Niu, J., & Wang, J. (2009). Characterization, ecological risk assessment and source diagnostics of polycyclic aromatic hydrocarbons in water column of the Yellow River Delta, one of the most plenty biodiversity zones in the world. *Journal of Hazardous Materials, 169*(1–3), 460–465.

Wang, C., Du, J., Gao, X., Duan, Y., & Sheng, Y. (2011). Chemical characterization of naturally weathered oil residues in the sediment from Yellow River Delta, China. *Marine Pollution Bulletin, 62*(11), 2469–2475.

Wang, C., Dao, X., Zhang, L. L., Lv, Y. B., & Teng, E. J. (2015). Characteristics and toxicity assessment of airborne particulate polycyclic aromatic hydrocarbons of four background sites in China. *Zhongguo Huanjing Kexue/China Environmental Science, 35*, 3543–3549.

Xie, W., Chen, A., Li, J., Liu, Q., Yang, H., & Lu, Z. (2012). County-scale distribution of polycyclic aromatic hydrocarbons in topsoil of the Yellow River Delta region. *Journal of Environmental Science and Health, Part A, 47*(10), 1419–1427.

Xue, B., Wang, Y., Zhang, D., Zhang, J., Leng, B., Huang, W., & Chen, Z. (2013). Concentration, distribution and sources of polycyclic aromatic hydrocarbons (PAHs) in surface sediments from Lijiang River, South China. *Bulletin of Environmental Contamination and Toxicology, 90*(4), 446–450.

Yang, H., Hsieh, L., Liu, H., & Mi, H. (2005). Polycyclic aromatic hydrocarbon emissions from motorcycles. *Atmospheric Environment, 39*(1), 17–25.

Yang, T.-T., Hsu, C.-Y., Chen, Y.-C., Young, L.-H., Huang, C.-H., & Ku, C.-H. (2017). Characteristics, sources, and health risks of atmospheric PM2.5-bound polycyclic aromatic hydrocarbons in Hsinchu, Taiwan. *Aerosol and Air Quality Research, 17*(2), 563–573.

Yim, U. H., Ha, S. Y., An, J. G., Won, J. H., Han, G. M., Hong, S. H., Kim, M., Jung, J.-H., & Shim, W. J. (2011). Fingerprint and weathering characteristics of stranded oils after the Hebei Spirit oil spill. *Journal of Hazardous Materials, 197*, 60–69.

Yunker, M. B., Macdonald, R. W., Vingarzan, R., Mitchell, R. H., Goyette, D., & Sylvestre, S. (2002). PAHs in the Fraser River basin: a critical appraisal of PAH ratios as indicators of PAH source and composition. *Organic Geochemistry, 33*(4), 489–515.